Monthly Notices of the ROYAL ASTRONOMICAL SOCIETY

MNRAS **545,** 1–7 (2026) https://doi.org/10.1093/mnras/staf2130
Advance Access publication 2025 November 29

First discovery of a fast-rotating blue straggler in a compact binary with a sub-stellar companion

A. H. Sheikh [1⋆], Biman J. Medhi,[1⋆] S. Messina [2], A. Subramaniam,[3] Neelam Panwar [4] and Ram Sagar[3]

[1]*Department of Physics, Gauhati University, Guwahati 781014, Assam, India*
[2]*INAF – Catania Astrophysical Observatory, via S. Sofia 78, I-95123 Catania, Italy*
[3]*Indian Institute of Astrophysics, Block II, Koramangala, Bangalore 560034, India*
[4]*Aryabhatta Research Institute of Observational Sciences, Manora Peak, Nainital 263002, India*

Accepted 2025 November 27. Received 2025 November 20; in original form 2025 July 31

ABSTRACT

We report the first discovery of a brown-dwarf (BD) companion using a radial velocity-based study of a rapidly rotating blue straggler star (BSS) in a short-period close binary system in NGC 2243. Multi-epoch spectra from VLT/FLAMES-GIRAFFE, analysed using ISPEC, yield stellar parameters for the primary: $T_{\rm eff} = 8800 \pm 700$ K, $Log(g) = 4.49 \pm 0.58$, [M/H] $= -0.31 \pm 0.15$, and $v \sin(i) = 95.63 \pm 9.78$ km s^{-1}. A Keplerian fit to multi-epoch radial velocity data reveals a nearly circular orbit ($e = 0.03 \pm 0.01$) with period $P = 0.234 \pm 0.007$ d, semi-amplitude $K = 4.79 \pm 0.05$ km s^{-1}, and systemic velocity $\gamma = 64.97 \pm 0.03$ km s^{-1}. The primary has a mass of 1.72 ± 0.12 M$_\odot$, radius 1.23 ± 0.22 R$_\odot$, and age of 0.51 ± 0.07 Gyr, while the orbital separation is 1.94 ± 0.05 R$_\odot$. The companion mass can range between 0.0199 and 0.099 M$_\odot$, depending on inclination; thus, the lightest BSS companion detected so far. The system is likely tidally synchronized, implying an inclination of $i = 21.08^\circ \pm 4.49^\circ$ and a companion mass of 0.056 ± 0.011 M$_\odot$, along with $T_{\rm eff}$ ∼1000–2500 K and radius of $\sim 0.08 \pm 0.13$ R$_\odot$, it is likely to be a BD. This is the shortest period binary known inside the BD desert for main-sequence stars, and one of the most compact sub-stellar companions ever identified in a stellar system. Single-star SED fitting and a *Gaia* Renormalized Unit Weight Error (RUWE) of 1.01 show no excess or astrometric anomalies, supporting a faint companion. This rare non-eclipsing BSS–BD system offers a valuable insight into the binary interaction during BSS formation.

Key words: methods: statistical – techniques: radial velocities – binaries: spectroscopic – blue stragglers – brown dwarfs.

1 INTRODUCTION

Blue straggler stars (BSSs) are classified as peculiar stars, brighter and bluer than the main-sequence turn-off (MSTO) point in a star cluster (A. R. Sandage 1953; A. H. Sheikh, B. J. Medhi & R. Sagar 2025). This is particularly puzzling, since the MSTO marks the evolutionary stage at which stars of similar mass and age start leaving the main sequence. Given that stars in a cluster are typically coeval, the presence of stars above the MSTO defies standard stellar evolution theories (A. H. Sheikh & B. J. Medhi 2024a,b). The primary formation mechanisms proposed to explain the formation of BSSs are: (a) BSSs may originate from close binary systems where mass transfer (MT) occurs as one star evolves, potentially leading to eventual merger (W. H. McCrea 1964); (b) they might result from direct stellar collisions or binary–binary interactions, processes more likely in the dense cores of globular clusters (J. G. Hills & C. A. Day 1976; A. Sills & C. D. Bailyn 1999; S. Chatterjee et al. 2013); and (c) the Kozai–Lidov mechanism in triple systems can shrink the inner orbit, eventually causing a merger within the inner binary system (H. B. Perets & D. C. Fabrycky 2009; S. Naoz & D. C. Fabrycky 2014). The dominant mechanism likely varies by environment; binary evolution, particularly MT, is thought to be the primary pathway in open clusters. MT can proceed via different evolutionary channels: Case A (during the main sequence), Case B (from a helium white-dwarf donor), or Case C (from a carbon–oxygen white dwarf), often involving common envelope (CE) phases that result in mergers (W. H. McCrea 1964; R. Kippenhahn, A. Weigert & E. Hofmeister 1967; R. F. Webbink 1976; X. Chen & Z. Han 2008a). Another possibility involves the coalescence of two MSTO stars during their evolution (V. V. Jadhav & A. Subramaniam 2021). Because multiple channels can lead to BSS formation, identifying the exact mechanism in individual cases remains complex. This requires detailed data, including chemical abundances, orbital characteristics, and evidence of companions.

An important but underexplored area is the role of sub-stellar companions, particularly brown dwarfs (BDs), in the formation and evolution of BSSs. BD, occupying the mass range between the heaviest planets and the lightest stars (∼13–80 M$_{\rm Jup}$), are rarely found as close companions to solar-type stars, a phenomenon known as the BD desert (D. Grether & C. H. Lineweaver 2006). This observational deficit of close-in BD companions suggests fundamental differences in how such systems form compared to typical stellar binaries. However, recent detections of extreme mass-ratio binaries involving possible BD companions have begun to challenge this view, offering

⋆ E-mail: asheikh@gauhati.ac.in (AHS); biman@gauhati.ac.in (BJM)

Table 1. Details of the spectroscopic observations of the BSS.

Epoch	Date of observations	MJD_{start}	MJD_{end}	SNR	RV km s^{-1}
1	2003-11-11	52954.30637961	52954.3259977512	46.31	61.99 ± 0.16
2	2003-11-12	52955.34357565	52955.3631937993	50.11	65.51 ± 0.15
3	2004-01-03	53007.22854852	53007.2481662989	42.24	60.02 ± 0.17
4	2004-01-03	53007.33201209	53007.3516299638	39.65	69.62 ± 0.17
5	2004-01-04	53008.12259351	53008.1422113352	43.92	63.13 ± 0.16
6	2004-02-17	53052.19710562	53052.2167234279	45.47	62.81 ± 0.17
7	2004-02-18	53053.13096882	53053.1505866082	40.51	63.85 ± 0.25
8	2004-03-03	53067.06653000	53067.0861478044	46.18	65.52 ± 0.17
9	2004-03-03	53067.18844213	53067.2080599575	34.84	64.63 ± 0.15
10	2004-03-04	53068.11941597	53068.1390336934	40.58	63.28 ± 0.21

new insights into binary evolution and accretion dynamics (K. G. Stassun, R. D. Mathieu & J. A. Valenti 2006). High-resolution spectroscopic studies of BSSs can provide critical clues about their origin, especially by detecting low-mass or sub-stellar companions. Binary systems with extreme mass ratios and short periods, especially those with rapidly rotating primaries, offer important insights into past MT history. In particular, the identification of very low-mass secondaries, possibly BD, in such configurations challenges standard binary evolution channels and provides constraints on the so-called BD desert. The presence of a BD in a close orbit with a BSS implies that sub-stellar objects can survive a CE phase, challenging assumptions that they are always destroyed or ejected during such violent events. Sub-stellar companions in BSS systems can reveal previously hidden binary configurations, which in turn alter our understanding of their mass-accretion history, binary demographics, and the range of viable evolutionary channels, especially across varying stellar environments.

In this work, we investigate a short-period binary system consisting of a BSS and a suspected BD [*Gaia* DR3 2893941099963718528, RA (α) = 97.°37960 and Dec. (δ) = −31.°34985] in NGC 2243, having a membership probability of 90.2 per cent with $G = 15.112 \pm 0.001$ mag, $G_{BP} = 15.192 \pm 0.001$ mag, $G_{RP} = 14.940 \pm 0.001$, $\pi = 0.2251 \pm 0.0247$ mas (A. H. Sheikh & B. J. Medhi 2024a). NGC 2243 is an old open cluster, approximately 3.67 Gyr old, at a distance of 3.65 Kpc. The existence of the BSS is known, whereas the existence of the BD is suspected. We determined the atmospheric parameters of this BSS as a single star from the spectral energy distribution analysis as $T_{eff} = 8000 \pm 125$ K, $Log(g) = 3.5$, $Log(L) = 1.025 \pm 0.001$ $L_{\odot}$, and $R = 1.681 \pm 0.52$ $R_{\odot}$ (A. H. Sheikh & B. J. Medhi 2024a). The remaining of the paper is organized as follows: Section 2 describes the data sets used in this study. The methodology is presented in Section 3. The results and discussion of this study are presented in Section 4.

2 DATA

BSS (*Gaia* DR3 2893941099963718528) was observed using the Fibre Large Array Multi Element Spectrograph (FLAMES) mounted on the Very Large Telescope (VLT) at the European Southern Observatory (ESO), located at Paranal Observatory in Chile. The observations were conducted with the GIRAFFE spectrograph in medium-resolution mode, as part of ESO program ID 072.D-0187(A). GIRAFFE was used with the HR9A set-up, providing spectral coverage from 509.5 to 540.4 nm at a resolving power of $R = 17,000$. Each exposure had an integration time of approximately 1695 s. In total, the BSS was observed across 10 different epochs, with a summary of the observations presented in Table 1. We have collected the data from the ESO Science Archive Facility.[1] As the data were already reduced in Phase 3, only sky subtraction and continuum normalization were performed, using the SPECUTILS PYTHON package.

3 METHODOLOGY

3.1 Radial velocity determination

To determine the radial velocities (RVs) of the primary star, we used an iterative cross-correlation approach. Each sky subtracted spectrum is first normalized to its continuum using the SPECUTILS PYTHON package. We then performed cross-correlation of each normalized spectrum against the first spectrum in the series, which was treated as an initial template. The resulting cross-correlation function (CCF) is calculated over a velocity range of ± 200 km s^{-1}, and the RV shift was obtained by fitting a one-dimensional Gaussian to the CCF peak. Using these initial RV measurements, we constructed a refined template by Doppler-shifting all spectra to the rest frame of the primary and median-stacking them. This procedure is repeated iteratively: at each iteration, a new template is generated and used for cross-correlation until the change in RVs between successive iterations falls below 0.01 m s^{-1}, ensuring convergence. Finally, to convert the relative RVs into an absolute scale, we cross-correlated the final median-stacked template with a synthetic atomic line mask appropriate for an A0-type star. The estimated RVs are listed in Table 1.

To identify periodic variations in the RV data, we used the Lomb–Scargle periodogram (W. H. Press & G. B. Rybicki 1989). We searched for periods ranging from 0.01 to 4 d by specifying a frequency range corresponding to these limits, to ensure accurate peak detection. The strongest signal is identified at a period of 0.234 $\pm$ 0.007 d. To assess the significance of this signal, we performed the false alarm probability (FAP) test using 1000 realizations of synthetic white noise, each generated at the same noise level as the observed RV uncertainties. The FAP for the best peak is found to be 0.001, indicating a highly significant detection. Additionally, we plotted horizontal lines on the periodogram corresponding to FAP levels of 0.1 per cent, 2 per cent, and 10 per cent, as shown in Fig. 1(a). The secondary significant (2 per cent) power peak corresponds to the second sub-harmonic of the strongest peak period. We also performed a bisector analysis of strong, unblended absorption lines between 516 and 533 nm to probe the source of the RV variations. All lines showed a bisector velocity span (BVS) of 0.000 km s^{-1}, indicating symmetric profiles. This rules out stellar activity or pulsations as the cause, supporting the interpretation that the RV variations arise from orbital motion, likely due to a companion.

[1] https://archive.eso.org/scienceportal/home

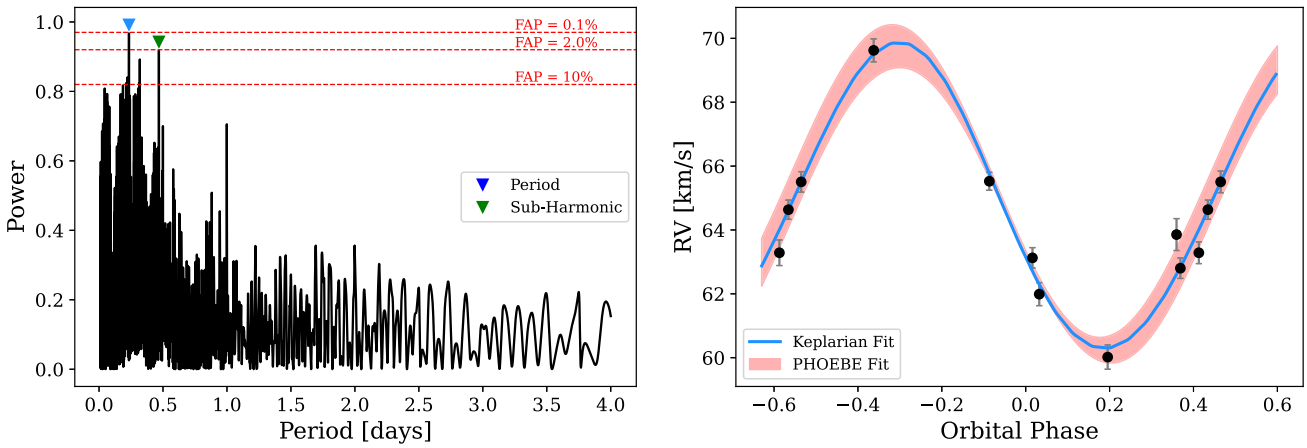

(a) (b)

Figure 1. (a) The Lomb–Scargle periodogram of the radial velocity measurements; (b) the phase-folded RV curve of the system. The black circles represent the observed RV data with error bars, and the blue solid curve shows the best-fitting Keplerian model derived from MCMC sampling. The red shaded region shows the best-fitting PHOEBE model for the range of BD parameters.

3.2 Radial velocity modelling

To model the observed RV variations caused by binary orbital motion, we adopt a standard Keplerian model. For a single-lined spectroscopic binary, the RV of the visible (primary) component as a function of time is given by

$$V(t) = \gamma + K\,[\cos(\omega + \nu(t)) + e\cos\omega]\,, \tag{1}$$

where γ is the systemic velocity of the binary, K is the RV semi-amplitude, ω is the argument of periastron, e is the orbital eccentricity, and $\nu(t)$ is the true anomaly at time t. The true anomaly $\nu(t)$ is related to the eccentric anomaly $E(t)$ through

$$\tan\left[\frac{\nu(t)}{2}\right] = \sqrt{\frac{1+e}{1-e}}\tan\left[\frac{E(t)}{2}\right] \tag{2}$$

and the eccentric anomaly $E(t)$ is obtained by solving Kepler equation

$$M(t) = E(t) - e\sin E(t), \tag{3}$$

where $M(t)$ is the mean anomaly, defined as

$$M(t) = \frac{2\pi}{P}(t - t_0), \tag{4}$$

where P is the orbital period and t_0 is the time of periastron passage.

To estimate the orbital parameters and their uncertainties, we employed a Markov chain Monte Carlo (MCMC) method using the EMCEE sampler (D. Foreman-Mackey et al. 2013). The orbital period is fixed at $P = 0.235 \pm 0.007$ d, based on the Lomb–Scargle periodogram analysis. We fit for five parameters: γ, K, e, ω, and t_0. In the MCMC sampling process, 100 walkers are used, along with 5000 iterations and 500 burn-in steps. We evaluated the Gelman–Rubin statistic ($\hat{R}$) for all estimated orbital parameters and found $\hat{R} = 1.01$, which indicates good convergence of the MCMC chains. The posterior distributions of the parameters are shown in Fig. 2. The best-fitting orbital parameters for BSS primary obtained from this method are listed in Table 2. We phase-folded the RV measurements using the orbital period P and reference time of periastron t_0, which maps the time series data on to a normalized phase space from 0 to 1. We fit the best-fitting Keplerian RV model derived from MCMC sampling, similarly folded in phase space to allow for direct

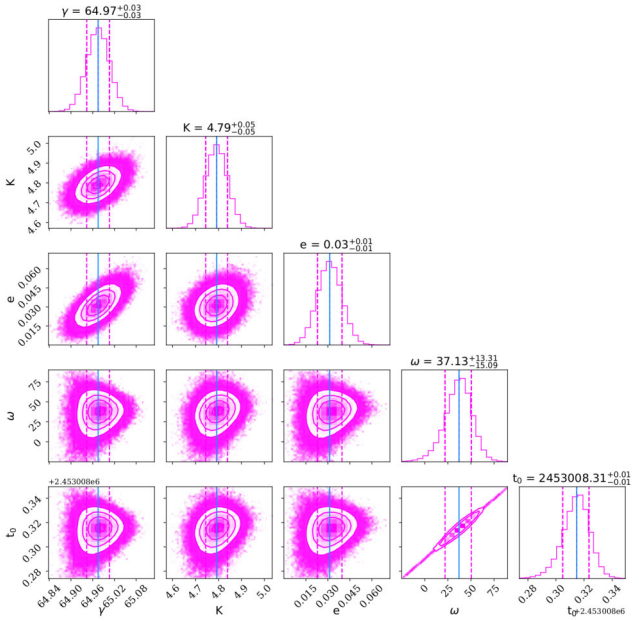

Figure 2. The posterior distributions of the estimated orbital parameters of the BSS primary. The blue solid line represents the median value (50th percentile), indicating the best-fitting parameter. The magenta dashed lines mark the uncertainty range, corresponding to the 16th and 84th percentiles.

comparison with the observed data as shown in Fig. 1(b). This phase-folded RV curve provides a clear representation of the orbital motion and demonstrates the periodic behaviour of the binary system. We classified the system as a single-lined spectroscopic binary (SB1).

3.3 Stellar parameter estimation of the components

3.3.1 Primary component

To estimate the atmospheric parameters of the BSS primary, we used the spectroscopic analysis tool ISPEC (S. Blanco-Cuaresma et al. 2014). It provides an integrated framework for detailed spectral

Table 2. The estimated best-fitting orbital parameters for the BSS primary.

γ (km s^{-1})	K (km s^{-1})	e	ω (deg)	t_0 (BJD)
64.97 ± 0.03	4.79 ± 0.05	0.03 ± 0.01	37.21 ± 14.22	2453008.31 ± 0.01

modelling. We adopted the synthetic spectral fitting technique, which involves generating synthetic spectra dynamically and fitting them to the observed data using a least-squares optimization algorithm. The synthetic spectra are generated using `ATLAS9.KuruczODFNEW` atmospheric models (F. Castelli & R. L. Kurucz 2003) and the MOOG radiative transfer code (C. Sneden 1973), both integrated within the ISPEC environment. Atomic line data are sourced from the *Gaia*–ESO Survey line list (U. Heiter et al. 2021), and we adopted solar reference abundances from N. Grevesse, M. Asplund & A. J. Sauval (2007). Fig. 3 shows the comparison between observed and synthetic spectra for the BSS primary. The synthetic spectrum (red) provides a good match to the observed spectrum (black), achieving a reduced chi-squared value of $\chi_r^2 = 0.037$ as shown in Fig. 3. The atmospheric parameters are derived in two steps, fitting first to Mg lines and then to Fe lines, independently. Initial values for the effective temperature ($T_{\rm eff} = 8000$ K), surface gravity ($Log(g) = 3.5$), and metallicity ([M/H] = –0.375) are adopted from A. H. Sheikh & B. J. Medhi (2024a). The microturbulence ($v_{\rm mic}$) and macroturbulence ($v_{\rm mac}$) velocities are estimated using empirical relations in ISPEC, yielding values of 4.11 and 22.97 km s^{-1}, respectively. The final atmospheric parameters for the BSS primary are listed in Table 3. We refrained from a detailed elemental abundance analysis due to the moderate spectral resolution ($R = 17,000$) and the high projected rotational velocity of the BSS, which causes significant line broadening and blending, especially in fast rotators, reducing measurement reliability.

Then the stellar mass and age of the BSS primary are estimated using PARAM 1.5,[2] a Bayesian tool based on MIST isochrones (L. da Silva et al. 2006; T. S. Rodrigues et al. 2017). The input parameters for this analysis included the spectroscopically determined $T_{\rm eff}$ and $Log(g)$, along with the near-ultraviolet (NUV) to infrared (IR) multi-band magnitude and parallax from *Gaia* DR3. These observables are used within the PARAM 1.5 framework to derive posterior probability distributions for the stellar properties. We then calculated the radius using the estimated mass and surface gravity. The resulting estimates of the mass, radius, and age are also listed in Table 3.

3.3.2 Secondary component

Since the primary BSS is an SB1, no information about the orbital motion of the companions is available; also, we could not find any signature of variability in *TESS* or other photometric timeseries. Therefore, only the mass function can be determined and is given by

$$f(M) = \frac{(M_s \sin i)^3}{(M_p + M_s)^2} = \frac{K^3 P}{2\pi G}(1 - e^2)^{3/2}, \tag{5}$$

where M_p and M_s are the masses of the primary and secondary companion, respectively. G is the gravitational constant. We estimate the minimum companion mass from the mass function, yielding $M_s \sin(i) = 0.0199 \pm 0.001$ M$_\odot$. Since the system is a close binary with an orbital period shorter than 0.3 d, tidal forces are expected to synchronize the stellar rotation with the orbital motion (S. Geier et al. 2010). This implies that the rotational period of the primary is equal to the orbital period. Assuming that the BSS primary is synchronized, its rotational velocity $v_{\rm rot}$ can be calculated as

$$v_{\rm rot} = \frac{2\pi R_p}{P}. \tag{6}$$

Given the projected rotational velocity, $v \sin(i) = 95.63 \pm 9.78$ km s^{-1} we derive an inclination angle of $i = 21.08^\circ \pm 4.49^\circ$. This corresponds to a companion mass of $M_s = 0.056 \pm 0.011$ M$_\odot$, placing it below the hydrogen-burning limit. This suggests that the companion is most likely a BD, supporting the scenario in which the BSS formed via MT from a sub-stellar companion in a close binary system. If we assume that the BSS primary is rotating at its break-up velocity, the inclination would be approximately $i \sim 11^\circ$, resulting in a maximum companion mass of ~ 0.099 M$_\odot$. So, the companion mass ranges from 0.0199 to 0.099 M$_\odot$. This is the smallest mass for a BSS companion, detected so far. This interpretation is further supported by the single-star SED fitting from A. H. Sheikh & B. J. Medhi (2024a), which shows no significant UV excess, an indication that there is no hot companion. Additionally, the *Gaia* Renormalized Unit Weight Error (RUWE) value of 1.01 indicates an excellent fit to a single-star astrometric model, with no signs of motion irregularities that would suggest the presence of a bright or massive companion. Together, these results are consistent with the presence of a very faint, low-mass companion, such as a BD, that does not significantly affect the photometric or astrometric profile of the system. Interpolating the properties of the BD companion using the ATMO2020 evolutionary models (M. W. Phillips et al. 2020) for ages between 0.1 and 5 Gyr, we estimate its physical parameters as listed in Table 4.

3.4 Tidal synchronization

The mechanism responsible for orbital synchronization in binaries remains debated. The orbit in this BSS + BD system is nearly circular ($e = 0.03$) with a very short period, indicating that tidal forces or a past evolutionary phase likely played a role in circularizing it. Under such conditions, the synchronization time-scale is expected to be short, and we can assume that the BSS rotation is synchronized with the orbital motion. However, whether the BSS is currently synchronized with the orbit depends on the efficiency of tidal interactions and the internal structure. To evaluate whether synchronization is physically plausible, we estimate the tidal synchronization time-scale using the J. P. Zahn (1977) formalism with dynamical tides for stars with convective cores and radiative envelopes

$$t_{\rm sync} = 52^{-5/3} \left(\frac{R_p^3}{G M_p}\right)^{1/2} \left(\frac{I}{M_p R^2}\right) \left(\frac{1+q}{q^2}\right)^{5/6} \times E_2^{-1} \left(\frac{a}{R}\right)^{17/2}, \tag{7}$$

where $q = M_S/M_p$, the mass ratio, a is the semimajor axis, and I is the moment of inertia of the BSS primary. E_2 is a tidal coefficient that is very sensitive to the structure of the star, especially the size of the convective core. We adopt $I/M_p R^2 \sim 0.077$ and $E_2 \sim 1.45 \times 10^{-8}$ from J. P. Zahn (1975). We calculated the semimajor axis using

[2] https://stev.oapd.inaf.it/cgi-bin/param

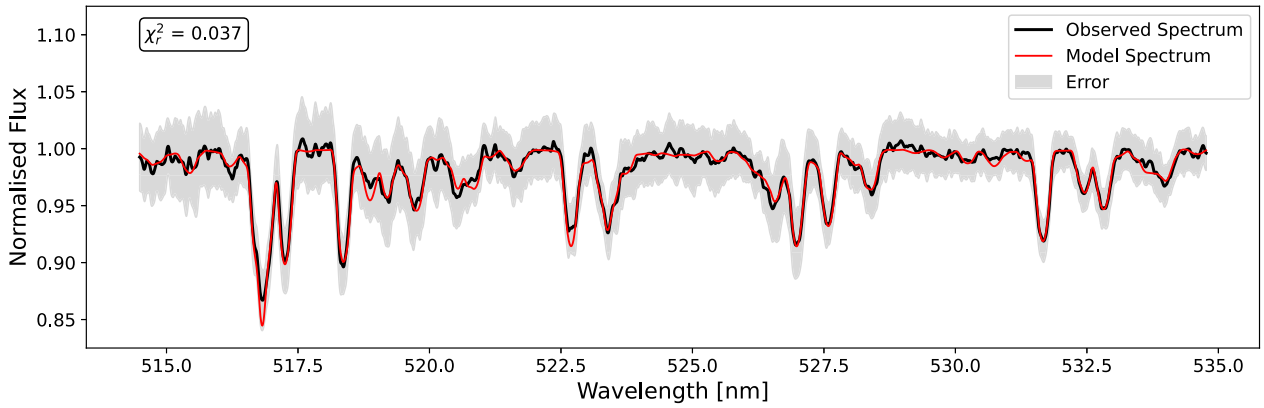

Figure 3. The synthetic spectral fitting of the BSS primary spectrum. The observed spectrum (in black) is shown with the best-fitting synthetic spectrum (in red).

Table 3. The estimated stellar parameters for the BSS primary.

$T_{\rm eff}$ (K)	$Log(g)$	(M/H)	$v \sin(i)$ (km s^{-1})	Mass ($M_\odot$)	Radius ($R_\odot$)	Age (Gyr)
8800 ± 700	4.49 ± 0.58	-0.31 ± 0.15	95.63 ± 9.78	1.72 ± 0.12	1.23 ± 0.22	0.51 ± 0.07

Table 4. The estimated stellar parameters for the BD companion.

$T_{\rm eff}$ (K)	$Log(g)$	Mass ($M_\odot$)	Radius ($R_\odot$)
$1100 - 2500$	$4.91 - 5.37$	0.056 ± 0.011	0.08 ± 0.13

Kepler's third law as $a = 1.94 \pm 0.05$ R$_\odot$. The synchronization time-scale is estimated to be $t_{sync} \sim 6000$ yr. For such a short-period system, this time-scale is reasonable.

We also estimate the tidal synchronization time-scale using the formalism of J.-L. Tassoul & M. Tassoul (1992), which describes an efficient hydrodynamical braking mechanism driven by tidally induced meridional currents in non-synchronous binary stars, leading to synchronization and circularization

$$t_{\rm sync} = 5.35 \times 10^{2+\gamma-N/4} \left(\frac{1+q}{q}\right) L^{-1/4} M_p^{5/4} R^{-3} P^{11/4}, \quad (8)$$

where the luminosity is given by $L = 4\pi\sigma R^2 T_{\rm eff}^4$. The parameter N accounts for energy transport in the outer stellar envelope and is assumed to be zero for stars with radiative envelopes. The parameter γ allows for deviations from synchronism and contributions from both binary components; we adopt $\gamma = 1.6$ following A. Claret, A. Gimenez & N. C. S. Cunha (1995). The synchronization time-scale for this formalism is also estimated to be $t_{sync} \sim 7000$ yr. This time-scale is extremely short compared to the evolutionary age of the BSS primary. Such a short time-scale indicates that the tidal forces would have been highly efficient in synchronizing the rotation of the primary with the orbital motion very early in the history of the system. Therefore, it is entirely reasonable to assume that the primary star is currently in a state of synchronous rotation with its orbit. However, given the small eccentricity and compact orbit, tidal forces are likely active, but the exact synchronization time-scale remains model-dependent and uncertain.

3.5 Binary modelling

To verify the estimated parameters of the BD component, we used the PHysics Of Eclipsing BinariE (PHOEBE) (A. Prša et al. 2016; K. E. Conroy et al. 2020). Since the primary RV curve alone is insufficient to constrain the system parameters, we used PHOEBE solely to assess whether the model can reproduce the observed RV curve. We tested the system under three configurations available in PHOEBE: detached, semidetached, and contact modes, using the parameters derived in the previous sections. Given the high temperature of the BSS primary and the low temperature of the BD secondary, we adopted appropriate values for the bolometric albedos and gravity-darkening coefficients: $[g_1 = 1, A_1 = 1]$ for the primary star, and $[g_2 = 0.32, A_2 = 0.5]$ for the secondary, respectively. For the limb-darkening coefficients of the BD secondary, we adopted values based on a blackbody approximation, due to the lack of reliable atmosphere models at such low temperatures. Among the tested configurations, the detached mode provided the best-fitting to the RV curve, as shown by the red shaded region representing the range of BD parameters in Fig. 1(b). The corresponding mesh diagram for the BSS + BD system in detached mode is shown in Fig. 4.

4 RESULTS AND DISCUSSION

The results obtained from this analysis are discussed as follows:

(i) The observed periodic RV variation with a best-fitting period of 0.234 ± 0.007 d and a semi-amplitude of $K = 4.79 \pm 0.05$ km s^{-1} provides strong evidence for a short-period binary system with a nearly circular orbit ($e = 0.03 \pm 0.01$). The high significance of this signal (FAP = 0.001) rules out noise as a cause. The clean bisector velocity span (BVS = 0.000 km s^{-1}) for multiple spectral lines confirms the stability and symmetry of the line profiles, ruling out stellar pulsations or magnetic activity. The system is clearly a single-lined spectroscopic binary, as no spectral contribution from a secondary component is detected.

(ii) The spectroscopic analysis using ISPEC revealed that the BSS primary is a hot, rapidly rotating star with: $T_{\rm eff} = 8800 \pm 700$ K, $\log g = 4.49 \pm 0.58$, [M/H] $= -0.31 \pm 0.15$, $v \sin(i) = 95.63 \pm 9.78$ km s^{-1}. Bayesian isochrone fitting yields: mass $= 1.72 \pm 0.12$ M$_\odot$, radius $= 1.23 \pm 0.22$ R$_\odot$, age $= 0.51 \pm 0.07$ Gyr. These values indicate a star that has been rejuvenated, i.e. relatively massive and young, likely due to past MT.

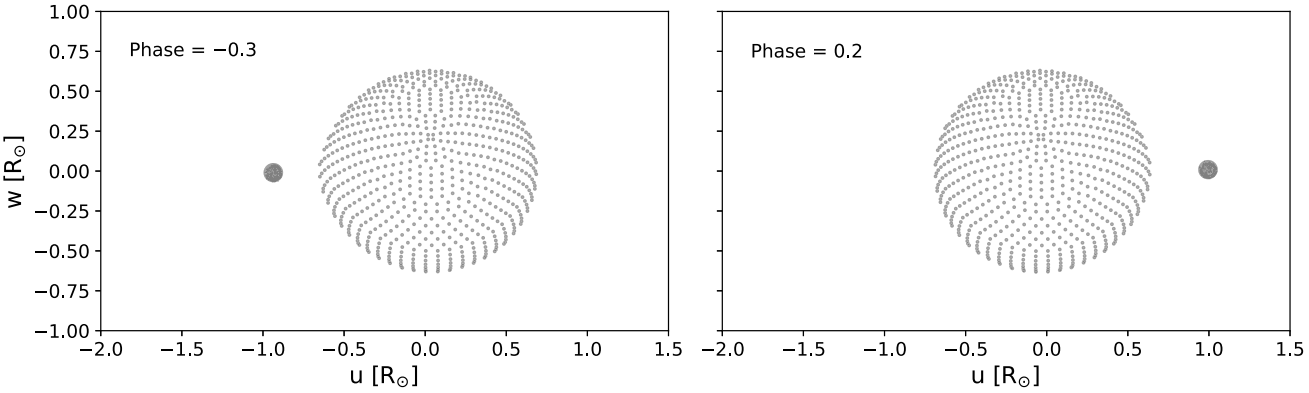

Figure 4. The mesh plot showing the BSS + BD binary system in different phases. The bigger object represents the BSS, whereas the smaller object represents the BD companion.

(iii) By assuming tidal synchronization and using the measured $v \sin(i)$ and the inferred rotational velocity from the orbital period, an inclination angle of $i = 21.08^\circ \pm 4.49^\circ$ is derived. This, combined with the RV-derived mass function, leads to a companion mass of 0.056 ± 0.011 $M_\odot$, below the hydrogen-burning limit, confirming that the companion is a BD. Alternatively, if we assume that the BSS primary is rotating at its break-up velocity, the inclination would decrease to approximately $i \sim 11^\circ$, resulting in a higher estimated companion mass of ~ 0.099 $M_\odot$, slightly above the hydrogen burning threshold. However, this extreme rotational assumption is inconsistent with the stability of the system. Therefore, we can confidently classify the companion as a BD.

(iv) Furthermore, SED fitting from UV to near-infrared (NIR) shows no excess flux, and the *Gaia* RUWE value of 1.01 indicates that there is no astrometric perturbation, supporting a low-luminosity companion. The absence of photometric variability is consistent with the low inclination and the faint, low-mass BD, which prevents transits and minimizes photometric effects. Adopting typical BSS parameters and using J. P. Zahn (1977) and J.-L. Tassoul & M. Tassoul (1992) formalism, the tidal synchronization time-scale is only a few thousand years, suggesting the system is likely synchronized. To verify these parameters, we used the PHOEBE to model the RV curve under detached, semidetached, and contact configurations. We found that the detached mode yielded the best match to the observed RV data.

The presence of a sub-stellar companion in a tight, nearly circular orbit around a BSS points to a non-standard formation pathway. Standard binary evolution cannot produce a BSS + BD system. In Case B/C MT, the remnant of an evolved ≥ 1 $M_\odot$ donor must be a He or CO WD rather than a BD (X. Chen & Z. Han 2008b; R. D. Mathieu & A. M. Geller 2009). Case A MT likewise cannot yield a BD companion, as the donor core becomes a He WD (O. G. Benvenuto & M. A. De Vito 2005), and a pure CE phase would likely destroy a BD if the stellar envelope is tightly bound (J.-C. Passy, M.-M. Mac Low & O. De Marco 2012). Thus, canonical two-body MT cannot explain the formation of a BSS with a BD companion.

External capture of a BD companion either through tidal capture or a three-body exchange is also highly unlikely in NGC 2243. Such encounters are intrinsically rare in old, low-density clusters, and NGC 2243 shows significant mass segregation, implying sub-stellar objects are depleted in the cluster core (A. H. Sheikh & B. J. Medhi 2024a). This further reduces the probability of BD capture. Moreover, close-in sub-stellar companions within $\sim$1 au are rarely removed by stellar encounters (M. S. Fujii & Y. Hori 2019; see also A. Bragaglia et al. 2001; M. B. Davies & S. Sigurdsson 2001), suggesting that the system formed and survived *in situ*. Together, these arguments strongly favour a primordial inner binary origin. High-precision RV surveys have long established the existence of a BD desert, with a striking paucity of BD companions within $\sim$ 3 au of FGKM type main-sequence stars (B. Campbell, G. A. H. Walker & S. Yang 1988; K. A. Murdoch, J. B. Hearnshaw & M. Clark 1993; G. W. Marcy & R. P. Butler 2000; D. Grether & C. H. Lineweaver 2006). Short-period MS + BD binaries with P<1 d are exceptionally rare, making our discovery of a BSS + BD system with a 5.6-h orbit right inside the so-called BD desert.

A plausible formation scenario is that the system originated as a hierarchical triple. In this picture, a distant tertiary evolved and transferred mass on to the inner star, creating the BSS, while the BD initially, the inner companion remained bounded. Kozai–Lidov oscillations can drive the inner binary to high eccentricity (S. Naoz & D. C. Fabrycky 2014; S. Naoz 2016), allowing tidal friction or merger-driven rejuvenation to form the BSS while preserving the BD in a short-period orbit. Subsequent tidal dissipation would circularize the system. It is therefore likely that the system originated with an evolved outer companion in a longer orbit. We suggest that the outer companion evolved and transferred mass to the BSS through merger, keeping the inner binary intact. It may be possible that the BD started off with a larger orbit, and the orbit shrank during MT. The system strongly resembles the hierarchical triple NGTS-7, where an M dwarf hosts a 16.2-h period BD companion and a wide tertiary (J. A. G. Jackman et al. 2019), but our BSS + BD binary is even more extreme: the BSS is more massive, and the BD orbit is significantly shorter. This makes it the shortest period binary known inside the BD desert, and one of the most compact sub-stellar companions ever identified in a stellar system. This BSS + BD system could be considered as the progenitor of systems such as the WD0837 + 185 system with a 4.2-h period with a BD in Praesepe (S. L. Casewell et al. 2012). The BSS, when it evolves, may go through a CE evolution and is likely to form a tight WD + BD system, several of which are known to date (P. R. Steele et al. 2013; S. L. Casewell et al. 2018; J. F. Wild et al. 2022).

The rarity of BD companions around main-sequence stars and the extreme orbital properties make this system a unique laboratory for studying triple-induced BSS formation and the survival of sub-stellar objects in close binaries. The presence of a BD companion around a BSS is rare, and to our knowledge, this is the first confirmed detection of a BSS–BD binary. To fully characterize the system,

continued variability monitoring and high-resolution spectroscopic follow-up are essential. This may provide tighter constraints on the orbital inclination, synchronization state, and chemical signatures of prior MT. Therefore, this system offers a valuable opportunity to refine models of binary evolution, to study triple-induced BSS formation, survival of BD in close binaries, and BD demographics in the BD desert.

ACKNOWLEDGEMENTS

We thank the anonymous referee for the valuable comments and suggestions that helped us to improve the quality of our paper. We made use of NASA's Astrophysics Data System as well as the VizieR and Simbad data bases at CDS, Strasbourg, France. The authors highly acknowledges the Department of Science and Technology (DST), Govt. of India, for providing the DST INSPIRE fellowship vide grant no. IF230175. This work is based on data obtained from the ESO Science Archive Facility with DOI(s): https://doi.org/10.18727/archive/27. We acknowledge the Inter-University Centre for Astronomy and Astrophysics, Pune, for providing access to the Pegasus HPC facility.

DATA AVAILABILITY

The data used in this paper will be made available upon reasonable request to the corresponding author.

REFERENCES

Benvenuto O. G., De Vito M. A., 2005, MNRAS, 362, 891
Blanco-Cuaresma S., Soubiran C., Heiter U., Jofré P., 2014, A&A, 569, A111
Bragaglia A. et al., 2001, AJ, 121, 327
Campbell B., Walker G. A. H., Yang S., 1988, ApJ, 331, 902
Casewell S. L. et al., 2012, ApJ, 759, L34
Casewell S. L. et al., 2018, MNRAS, 476, 1405
Castelli F., Kurucz R. L., 2003, in Piskunov N., Weiss W. W., Gray D. F., eds, Modelling of Stellar Atmospheres. Vol. 210, Proc. IAU Symp., p. A20
Chatterjee S., Rasio F. A., Sills A., Glebbeek E., 2013, ApJ, 777, 106
Chen X., Han Z., 2008a, MNRAS, 384, 1263
Chen X., Han Z., 2008b, MNRAS, 387, 1416
Claret A., Gimenez A., Cunha N. C. S., 1995, A&A, 299, 724
Conroy K. E. et al., 2020, ApJS, 250, 34
da Silva L. et al., 2006, A&A, 458, 609
Davies M. B., Sigurdsson S., 2001, MNRAS, 324, 612
Foreman-Mackey D., Hogg D. W., Lang D., G. J., 2013, PASP, 125, 306
Fujii M. S., Hori Y., 2019, A&A, 624, A110
Geier S., Heber U., Podsiadlowski P., Edelmann H., Napiwotzki R., Kupfer T., Müller S., 2010, A&A, 519, A25
Grether D., Lineweaver C. H., 2006, ApJ, 640, 1051
Grevesse N., Asplund M., Sauval A. J., 2007, Space Sci. Rev., 130, 105
Heiter U. et al., 2021, A&A, 645, A106
Hills J. G., Day C. A., 1976, ApJ, 17, 87
Jackman J. A. G. et al., 2019, MNRAS, 489, 5146
Jadhav V. V., Subramaniam A., 2021, MNRAS, 507, 1699
Kippenhahn R., Weigert A., Hofmeister E., 1967, Methods Comp. Phys., 7, 129
Marcy G. W., Butler R. P., 2000, PASP, 112, 137
Mathieu R. D., Geller A. M., 2009, Nature, 462, 1032
McCrea W. H., 1964, MNRAS, 128, 147
Murdoch K. A., Hearnshaw J. B., Clark M., 1993, ApJ, 413, 349
Naoz S., 2016, ARA&A, 54, 441
Naoz S., Fabrycky D. C., 2014, ApJ, 793, 137
Passy J.-C., Mac Low M.-M., De Marco O., 2012, ApJ, 759, L30
Perets H. B., Fabrycky D. C., 2009, ApJ, 697, 1048
Phillips M. W. et al., 2020, A&A, 637, A38
Press W. H., Rybicki G. B., 1989, ApJ, 338, 277
Prša A. et al., 2016, ApJS, 227, 29
Rodrigues T. S. et al., 2017, MNRAS, 467, 1433
Sandage A. R., 1953, AJ, 58, 61
Sheikh A. H., Medhi B. J., 2024a, AJ, 168, 274
Sheikh A. H., Medhi B. J., 2024b, MNRAS, 534, 4031
Sheikh A. H., Medhi B. J., Sagar R., 2025, ApJ, 989, 16
Sills A., Bailyn C. D., 1999, ApJ, 513, 428
Sneden C., 1973, ApJ, 184, 839
Stassun K. G., Mathieu R. D., Valenti J. A., 2006, Nature, 440, 311
Steele P. R. et al., 2013, MNRAS, 429, 3492
Tassoul J.-L., Tassoul M., 1992, ApJ, 395, 259
Webbink R. F., 1976, ApJ, 209, 829
Wild J. F. et al., 2022, MNRAS, 509, 5086
Zahn J. P., 1975, A&A, 41, 329
Zahn J. P., 1977, A&A, 57, 383

This paper has been typeset from a TEX/LATEX file prepared by the author.